



Enhancing Legged Robot Navigation of Rough Terrain via Tail Tapping

Daniel Soto¹(✉), Kelimar Diaz², and Daniel I. Goldman²

¹ School of Mechanical Engineering, Georgia Tech, Atlanta, GA 30332, USA
daniel.goldman@physics.gatech.edu

² School of Physics, Georgia Tech, Atlanta, GA 30332, USA

Abstract. Legged systems offer benefits over their wheeled counterparts in their ability to negotiate rugose and heterogeneous environments. However, in rough terrain, these systems are susceptible to failure conditions. These failures can be avoided through different strategies such as environmental sensing or passive mechanical elements. Such strategies come at an increased control and mechanical design complexity for the system, often without the capability of failure recovery. Here, we sought to systematically investigate how contact generated from a tail can be used to mitigate failures. To do so, we developed a quadrupedal C-leg robophysical model (length and width = 27 cm, limb radius = 8 cm) capable of walking over rough terrain with an actuated tail (length = 17 cm). We programmed the tail to perform three distinct strategies: static pose, periodic tapping, and load-triggered (power) tapping, while varying the angle of the tail relative to the body. We challenged the robot to traverse a nearly impassable terrain (length = 160 cm, width = 80 cm) of randomized blocks with dimensions scaled to the robot (length and width = 10 cm, height = 0 to 12 cm). Without the tail, the robot was often trapped among blocks, limiting terrain traversal, independent of gait pattern. With the tail, the robot could still be trapped due to complex interactions (difficult to detect or predict) between the system and its immediate surroundings. However, using the tail, the robot could free itself from trapping with a probability of 0 to 0.5, with the load-driven behaviors having comparable performance to low frequency periodic tapping across all tail tapping angles. By increasing the probability of freeing, the robot was more likely to traverse the rough terrain (mean distance before failure of 1.47 to 2.49 body lengths). In summary, we present a framework that leverages mechanics via tail-ground interactions to mitigate failure and improve legged system performance in heterogeneous environments.

Keywords: Rough terrain · Locomotion · Robot · Quadruped · Tail · Failures

1 Introduction

Field robots can face unstructured, heterogeneous environments such as those in Fig. 1A and B. Therefore, they must be equipped with methods to handle and

traverse such terrains. In general, there are two main strategies to do so: environmental mapping and passive mechanical elements. Environmental mapping relies on external feedback to find footholds or secure locations [1] to place feet in order to avoid areas where the robot could fail and be damaged. This strategy is referred to as task-space closed loop because the robots use external environmental information to actively compensate for obstructions by avoiding them or through careful support placement. Some examples of robots employing such a strategy that are successful in various environments are Spot [2] and Atlas [3]. The drawback of this method, however, is that it requires complex control and actuation, with robust sensors, to be able to traverse most environments.

In contrast, the second strategy does not require the same level of complexity or control to achieve comparable performance. Instead, passive mechanical elements are used to augment a robust system with simple underlying motion and control. This strategy has been implemented in a variety of robots. The robotic hexapod RHex [4], inspired by cockroach locomotion, relies on compliant limbs and a clock-driven motion profile to traverse uneven terrain. Furthermore, compliant C-legs were implemented on RHex to improve its ability to climb over obstacles [5] and distribute the mechanical feedback at the limbs [6]. Additionally, directionally compliant limbs have improved the performance of a centipede robot on rough terrain [7], and a snake robot with muscle-like morphology and actuation traversed multi-post arrays via emergent passive mechanics [8].

Despite the benefits from mechanics-focused designs and task-space methods, robots can still be susceptible to failure conditions in complex terrains due to size/design. In unstructured environments (Fig. 1A and B), the size of the robot plays an important role. Large walkers can clear gaps and obstacles but can collapse an underlying structure or tip over. In contrast, small walkers are less likely to clear gaps or obstructions. There is a moderate size and weight class where the robot is unlikely to collapse a structure, be damaged from falling, and has the potential to clear obstacles and gaps. However, this “middle” category of robots can have limb dimensions that are of comparable size to the obstructions and holes being traversed [9]. In this regime, “trapping” begins to occur [6] where a limb falls into a cavity and the robot is unable to exit. This form of locomotor failure is detrimental to robots following either movement strategy and can be encountered across many environments, such as those in Fig. 1A and B.

This problem suggests that either the limbs must be improved to be actively adaptable, or a simpler actuated mechanism, such as a tail, can be introduced to mitigate failures and recover before damage occurs. Other robotic studies have shown improved locomotor performance with the addition of a tail [10–12]. For instance, TailBot, a wheeled robot, relied on a rigid tail contacting the ground to limit pitch and negotiate obstacles [13]. Additionally, active tail-ground contact can induce steering in legged systems [14]. We posit a tail performing ground contact can also address the problem of trapping.

Thus, in this paper, we built an open-loop robophysical model with an attachable tail and challenged it to traverse a terrain of randomized blocks with dimensions scaled to the robot. We tested three different tail tapping strategies and

noted how these strategies influenced the robot’s performance. Specifically, we examined the robot’s ability to free itself from trapping and the total distance it traveled before it was unable to free itself. We found that, when used appropriately, a tail improved the probability of freeing and increased the likelihood of terrain traversal. This suggests that a simple limb-uncoordinated tail can be used to aid existing robot designs and act as an “emergency mechanism” when exploring hazardous environments to mitigate damage and assist traversal.

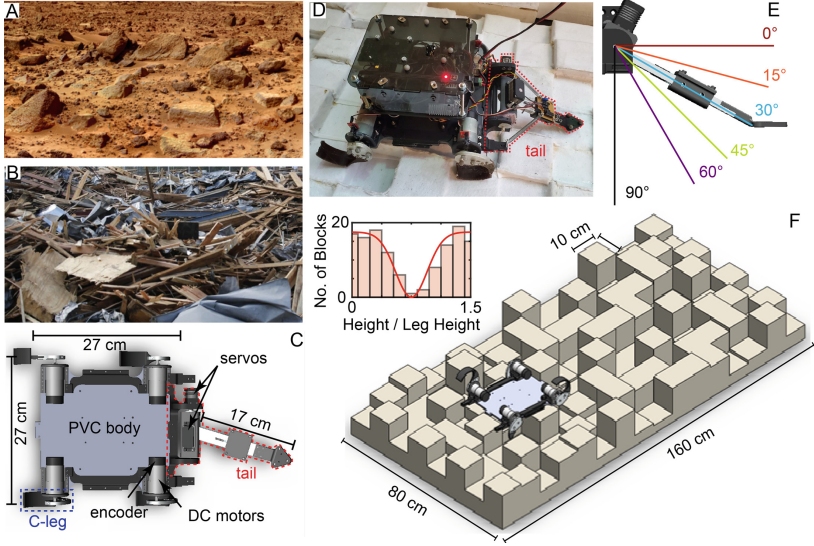


Fig. 1. Robot and rough terrain. (A) Martian landscape [15]. (B) Rubble after building collapse [16]. (C) Design of robophysical model with annotations highlighting key elements. (D) Robophysical model with tail. Red dashes outline the tail. (E) Side view of the robot tail with varied tail angle β_{set} - 0° (red line), 15° (orange line), 30° (blue line), 45° (green line), 60° (purple line), and 90° (black line). (F) Design of terrain with simplified robot model.

2 Materials and Methods

Inspired by RHex’s capabilities in rough terrain, we built a quadrupedal robophysical model shown in Fig. 1. We opted for four legs rather than six to gauge the challenges and capabilities associated with a “minimal RHex” design. The robot consisted of a PVC base with an acrylic top (length and width = 27 cm, height = 16 cm, mass = 2.8 kg) with four C-legs actuated by DC motors (operated at 12V, max torque of 27 kg-cm). Each C-leg consisted of an aluminium mount and a rubber C-shaped pad (width = 3 cm, radius = 8 cm, 3 mm thick). Hot glue was added to the outer portion of the rubber leg to improve traction. Legs were actuated via a microcontroller (Arduino Due). In addition, each DC

motor used an encoder to track angular position and was mounted alongside a photo-interrupter to mitigate encoder drift.

Each leg was controlled to rotate according to an angular trajectory known as the Buehler Clock [4], which consists of a fast and a slow region (Fig. 2A), and the overall system walks by following a gait pattern (i.e. phasing the limbs relative to each other in time) [17]. An example pattern for a diagonal couplet gait is shown in Fig. 2B, where the symmetric phasing (phasing between limbs on the same side) (ψ_{lat}) is 0.35 and the asymmetric phasing (phasing between the pairs of limbs on either side) (ψ_{opp}) is 0.50. Each motor followed the assigned motion profile via a feedback control scheme detailed in Fig. 2C. To prescribe different gait patterns, state feedback control was used on the phasing of each limb relative to another. The output of this controller adjusted the setpoint velocity for each limb. To ensure that failure events did not cause permanent damage, we implemented a “kill” switch on the robot. If a limb failed to complete a revolution within two gait cycles (5 s), the robot shut down and the trial ended.

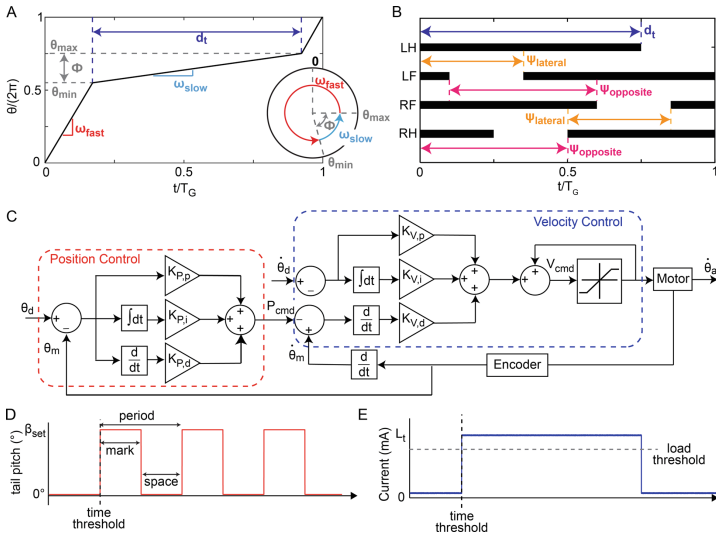


Fig. 2. Control schemes. (A) Motion profile for limb rotation. Trajectory is (black line) described by two rotational speeds: fast (red) and slow (blue). The slow region is described by the stance phase (gray) and the time spent there is described by the duty factor (purple). (B) Gait diagram showing relative limb phasing. Black is when the limb is in the slow region and has a length equal to the duty factor (purple). Each lateral and opposite pair is phased by ψ_{lat} (orange) and ψ_{opp} (pink), respectively. (C) Control scheme for a single limb where θ_m and θ_d are the measured and desired positions, respectively. (D) Diagram showing rectangular wave used to drive periodic tapping. “Mark” and “space” describe the duration of the wave at β_{set} and 0° , respectively. (E) Diagram showing expected behavior of load versus time during a trapping event.

To model nearly impassable (without careful planning) terrains, we built a stepfield of blocks (length = 160 cm, width = 80 cm) with a random distribution of heights, a known approach for modeling rough terrains [4, 18, 19] (Fig. 1F). For our study, we deliberately designed this course to cause trapping. To do so, the individual blocks were scaled to the length of the legs (length and width = 10 cm). Block heights were determined by a flipped Gaussian distribution with a mean of 6 cm (0.75 leg radius) and standard deviation of 2 cm (0.25 leg radius) (Fig. 1F inset). This ensured large height differences between adjacent blocks. Individual blocks were made out of insulation foam glued on a wooden surface and covered with a thin wooden square (3 mm thick) to prevent damage to the foam interior.

To study whether non-propulsive mechanics can aid navigation on rough terrain, we developed an actuated tail (length = 17 cm, width = 2.7 cm, weight = 0.4 kg) (Fig. 1D). The tail consisted of an aluminum beam with a triangular pad for ground contact. The tail was actuated along the pitch and yaw directions via two servo motors (operated at 7.4 V, max torque of 40 kg-cm). Tail movement was actively driven along the pitch direction, varying the maximum tail angle (β_{set}) relative to the robot body from 0° to 90° (Fig. 1E). Movement along the yaw direction was passive, allowing the tail to move side-to-side. Restorative springs were used such that the tail returned to the center after such movement.

We prescribed three tail strategies: static tail, periodic tapping, and load-triggered tapping. The static tail strategy consisted of maintaining a constant angle relative to the body. This method can provide support in locomoting systems, where single disturbances cause pitch instabilities that can lead to failure [13]. Periodic tapping consisted of tail oscillations from 0° to β_{set} , driven by a rectangular wave with a frequency chosen before each trial (Fig. 2D). Tapping frequencies were varied for different β_{set} by changing the space between pulses in the rectangular wave (mark was kept constant at 0.25 s). With this strategy, the tail tapped at the set frequency irrespective of whether it made ground contact. Load-triggered tapping relied on failure detection and recovery. We expected a large, sustained increase in the current drawn when the robot encountered failure. Thus, the tail moved to β_{set} when the load exceeded a threshold for a given time threshold (Fig. 2E).

For all trials detailed in this paper, we set the duty factor at 0.75 and the gait period at 2.5 s. We recorded the robot's path over the terrain via two webcams, a side view and top view. The center of geometry of the robot (without the tail) was tracked via Optitrack and analyzed with custom MATLAB functions. We discarded trials where the robot went off the sides of the course and ended tests once they achieved a displacement of 140 cm. We did not actively control the heading; instead, we studied the emergent properties of the walker with fixed limb dynamics (gaits). Trials were conducted until at least 4 trials (maximum of 17) were obtained where the robot did not fall off the course or suffer damage. We examined the likelihood of traversal by plotting each behavior's empirical complementary cumulative distribution function (CCDF) of the final displacement from each trial. We obtained the mean displacement before failure (MDBF) by

integrating the curve of the CCDF. In addition, we calculated the probability of freeing by taking into account each trapping and freeing event. We searched for instances of sticking and calculated the probability of freeing by subtracting the last sticking event (where the robot failed, if applicable) from the total number of times the robot was stuck. Then, the value was divided by the total number of sticking events.

3 Results

We first tested the performance of the tailless robophysical model using distinct gaits (pace, single foot, diagonal couplet, trot, prnk, and bound) over a flat surface and the rough terrain. Displacement over time and example trajectories for each gait are shown in Fig. 3A, C, E, and B, D, F on flat and rough terrain, respectively. On the flat surface, the robot could traverse the course independent of the prescribed gait (Fig. 3C). Only with the diagonal couplet gait was the robot able to reach the end of the course consistently. With the other gaits, the robot did not move in a straight path and fell off the sides. However, the robot did not exhibit any failure (such as trapping) with any of the gaits. On the rough terrain, the robot was often trapped between blocks, hindering it from traversing the course (Fig. 3D, F). Median displacement traveled for each of these gaits on both terrains is shown in Fig. 3G. Indeed, a simple open-loop limb control was not sufficient to mitigate and recover from failures caused by the terrain. For the following experiments with the actuated tail, the robot used the diagonal couplet gait since it was the only gait that remained within the course bounds and reached the end of the course every run.

For all tail strategies, only the pitch servo (along the vertical plane) was active and the yaw servo (along the horizontal plane) was free to move passively. For the static tail strategy, β_{set} was 0° , 15° , 30° , and 45° . Figure 4A shows sample trajectories for each angle. Independent of β_{set} , the robot occasionally became stuck in the rough terrain. This is observed in the displacement of the robot over time, where the absolute displacement plateaued once the robot became stuck (Fig. 4B–E). Calculating the CCDF for each β_{set} , we discovered that 30° displayed a higher probability of traversing the rough terrain, in comparison to β_{set} of 0° , 15° , and 45° as well as the robot without the tail (Fig. 4F). In addition, we found that the probability of freeing was 0.25, 0.13, 0.08, 0.31, and 0.36 for no tail, 0° , 15° , 30° , and 45° , respectively (Fig. 4G). When the tail contacted the surface, it could restrict the ability for the limbs to free the robot if it was in a trap. This was observed when the tail had a β_{set} of 0° and 15° . When β_{set} was 30° and 45° , the tail-ground contact was frequent and offered support for the robot, preventing the back limbs from falling into holes. However, when β_{set} was 45° , the front was pushed further down, making it more likely to collide with the terrain blocks. This high tail angle also exposed more of the tail to the terrain at a large impact angle, making instances of the tail getting caught on a block edge more common.

For the second tail strategy, we tested periodic tapping and varied β_{set} to 15° , 30° , and 45° . We tested a high and a low frequency per angle. This helped

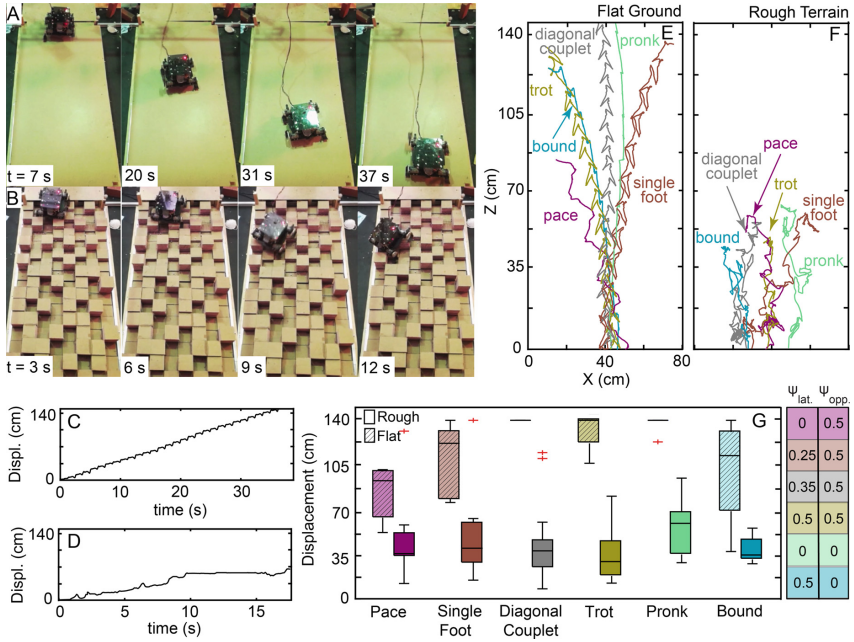


Fig. 3. Gait trials over flat and rough terrain. Snapshots of the robot moving over a flat (A) and rough (B) terrain, using the diagonal couplet. Example displacement over time for the robot using the diagonal couplet gait over flat (C) and rough (D) terrain. Example trajectories for each gait over flat (E) and rough (F) terrain. Gaits tested were pace (purple), single foot (burgundy), diagonal couplet (gray), trot (gold), pronk (turquoise), and bound (blue). (G) Median displacement per gait over flat and rough terrain. Red crosses show outliers. Phase shift between lateral (ψ_{lat}) and opposite (ψ_{opp}) limbs for each gait are shown to the right.

to determine the effects that tap amplitude and timing have on the robot's performance. For each angle, we maintained the max frequency of 2 Hz. For the low frequency tests, we chose a different frequency for each angle to account for the different associated amplitudes. The results for these behaviors are shown in Fig. 5. Across all angles tested, the less frequent tapping outperformed the high frequency tapping. This is seen in the example trajectories in Fig. 5A–B and the displacement over time in Fig. 5C–E all showing the low frequency trial outperform its high frequency counterpart. When tail-ground contact was made, high frequency tapping could free the robot but ultimately caused it to fall off the course. In addition, the high frequency taps caused the robot to jostle in the terrain when it was trapped, leading to further trapping. This behavior led to a decreased likelihood of traversal in comparison to the robot without the tail (Fig. 5G). We found that the probability of freeing was 0.17 for a β_{set} of 15° , whereas at a β_{set} of 30° and 45° , the robot could not free itself if it was stuck (Fig. 5H). On the other hand, the method of less frequent tapping

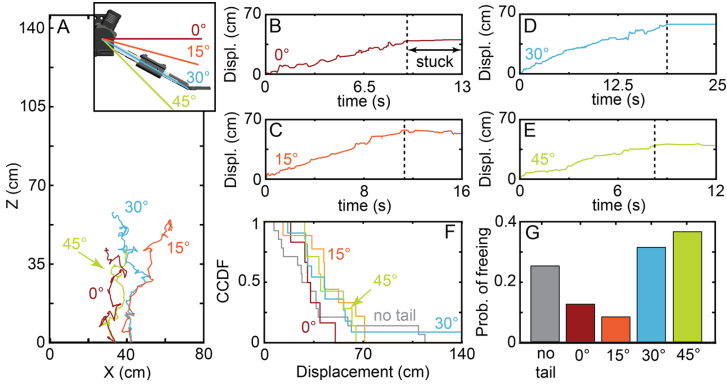


Fig. 4. Static tail strategy. (A) Example trajectories over rough terrain for each angle tested: 0° (red), 15° (orange), 30° (blue), and 45° (green). Example displacements versus time for β_{set} of (B) 0° , (C) 15° , (D) 30° , and (E) 45° . Black lines indicate where the final trapping event occurred. (F) Complementary cumulative distribution functions (CCDFs) and (G) probability of freeing for each tested angle and the robot without the tail (gray).

had a likelihood of traversing the terrain comparable to or greater than that of the robot without the tail (Fig. 5F). In addition, we found a probability of freeing of 0.11, 0.42, and 0.50 for a β_{set} of 15° , 30° , and 45° , respectively. With a lower tapping frequency, a β_{set} of 15° did not have sufficient amplitude to guarantee tail-ground contact. However, at β_{set} of 30° and 45° , the tail made consistent ground contact, improving the overall performance. At these angles, the tail tended to tap whenever the robot was on the verge of failure. We note that the tail often freed the robot by doing a single tap and it landed in a new region where it became trapped. Once there, the robot typically reached the kill condition before a new series of taps could be performed to free the device. The improvement observed with the low frequency, high amplitude tests suggests the optimal timing of those taps changed with regards to where the robot was located in space and where it was within its gait pattern. For the final tail strategy, we tested load-triggered tapping where we varied β_{set} to 30° , 60° , and 90° . Once the measured current exceeded the load and time thresholds, the tail began tapping at its maximum frequency until the detected load dropped below the threshold, after which the tail finished its last cycle before resting (see Fig. 2D, E). Figure 6A shows sample trajectories of each tail tapping angle. Independent of β_{set} , the load-triggered tapping strategy managed to address stuck cases as they occurred, best seen in the example displacements in Fig. 6B–D at times 9.5 s, 12 s, and 9 s, respectively. This improvement is reflected in the likelihood of terrain traversal being comparable to or greater than the robot without the tail (Fig. 6E). This strategy resulted in a freeing probability of 0.28, 0.40, and 0.35 for β_{set} of 30° , 60° , and 90° , respectively. When β_{set} was 60° , we observed the greatest improvement across all metrics. While a β_{set} of 90° had

comparable likelihood to 60° of traversing the terrain, there was a decrease in the probability of freeing. We posit the robot was over-disrupted by the large tapping amplitude, causing the device to jostle and change its heading in the terrain, leading to additional trapping that did not have guaranteed tail-ground contact.

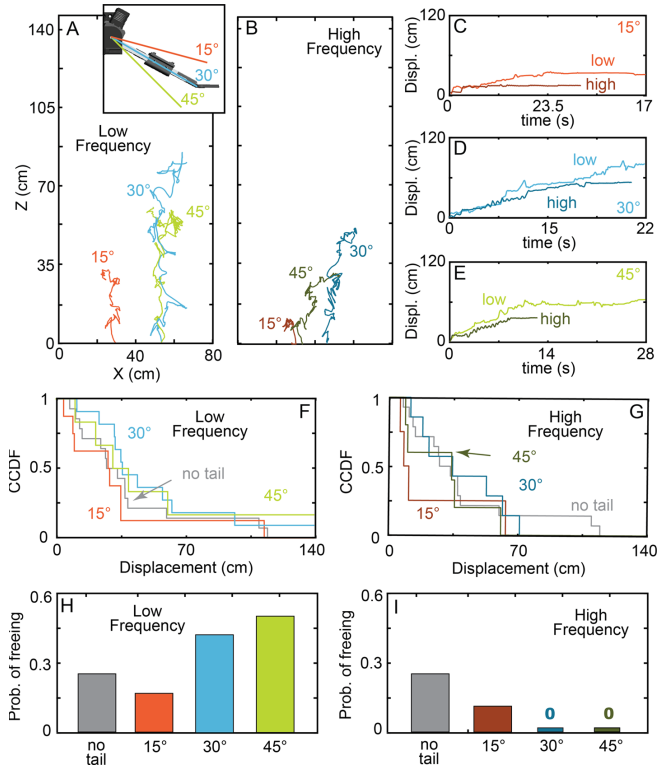


Fig. 5. Periodic tapping strategy. Example trajectories over rough terrain for periodic tapping at (A) low and (B) high frequency. Inset in (A) shows angles tested: 15° (orange), 30° (blue), and 45° (green). Higher frequency tapping colored with a darker shade of the assigned color. Example periodic tapping displacements versus time for (C) 15° , (D) 30° , and (E) 45° . CCDFs for tested angles in (F) low and (G) high frequency with the robot without the tail (gray). Probability of freeing for each angle for low (H) and high frequency (I).

4 Discussion

Without the use of a tail, the robot had difficulty and could not fully traverse the rough terrain (Fig. 3D), independent of the prescribed gait. This was due to robot-terrain interactions in the device's immediate surroundings that led to

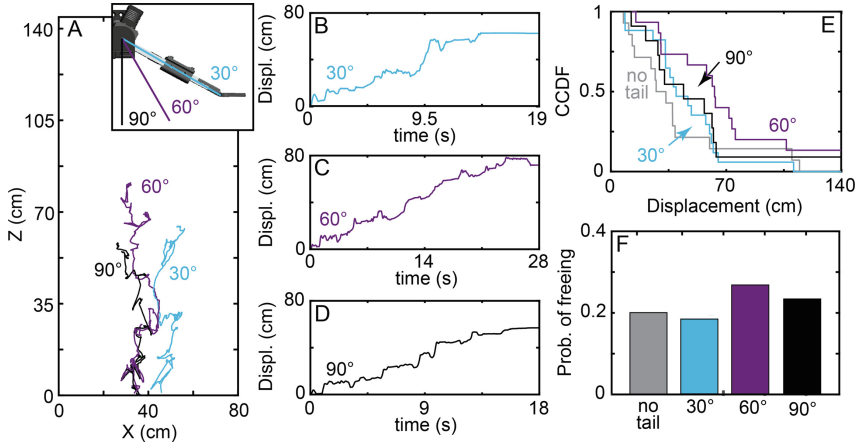


Fig. 6. Load-triggered tapping strategy. (A) Example trajectories over rough terrain for each angle tested for the load-triggered behavior. Inset illustrates angles tested: 30° (blue), 60° (purple) and 90° (black). Example displacements versus time for (B) 30°, (C) 60°, and (D) 90°. (E) CCDFs for each tested angle and the robot without the tail (gray). (F) Probability of freeing for each angle.

trapping. This suggests that terradynamic interactions over heterogeneous environments of this complexity and scale are difficult to predict and resolve. However, through the use of a tail to contact the terrain, the likelihood of traversal and freeing could be improved. Comparing across all the behaviors, we found that low frequency periodic tapping at β_{set} 30° and 45° outperformed other tail strategies with a probability of freeing of 0.42 and 0.50, respectively (Fig. 7A). This strategy also improved the likelihood of traversal, having a mean distance before failure (MDBF) of 1.93 body lengths (BL) and 1.87 BL, respectively (Fig. 7B). This was an improvement in comparison to the robot without the tail (MDBF of 1.47 BL, freeing probability of 0.25). However, this periodic strategy is non-advantageous outside of a lab setting. In reality, the robot only needs to tap momentarily to free itself from a trap. Disruptions brought on by further tapping could hinder performance over less hazardous areas. In contrast, load-triggered tapping and a static tail both offer real-world applicability. For the static tail, the MDBF increased to 1.85 BL and 1.72 BL and the probability of freeing to 0.31 and 0.36 for 30° and 45°, respectively. Furthermore, in real-world settings, this behavior can also offer benefits in homogeneous or less hazardous environments by stabilizing the system through a new point of support. For load-triggered tapping, the probability of freeing increased from 0.25 (no tail) to 0.28, 0.40, and 0.35 for β_{set} of 30°, 60°, and 90°, respectively. Each angle also exhibited higher MDBFs than the robot without a tail (1.68 BL, 2.49 BL, and 1.86 BL, respectively). We posit this strategy is desirable for field robotics since it will only begin tapping once a “failure” threshold is met, avoiding needless disruptions to the system. When properly actuated, an active tail offers benefits

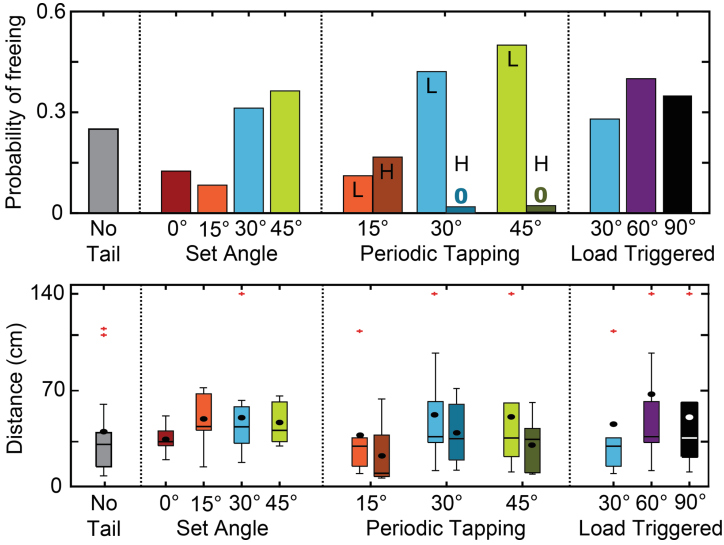


Fig. 7. Tail-use strategies comparison. (A) Probability of freeing for each behavior. (B) Median displacement for each tail behavior. Black/white dots show the mean displacement before failure (MDBF). Black/white horizontal lines show the median. Red crosses show outliers. Statistic performed with a Wilcoxon rank sum test, comparing each behavior. Differences were significant at $p \leq 0.05$ when comparing load-triggerged 60° to low frequency 15°, high frequency 15°, and high frequency 45°.

in negotiating complex environments, particularly at β_{set} of at least 30°. We also demonstrated that, if improperly implemented, a tail could hinder the robot and its ability to explore such terrains, as is the case for high frequency tapping and β_{set} less than 30°.

5 Conclusion

In this study, we investigated failure dynamics of a moderate-sized legged robot negotiating an unstructured environment. We posit that robots of this size can serve as payload carriers or scouts over similar terrains, having the potential to clear most of the obstructions and gaps. However, such robots are faced with trapping conditions, often without recovery methods. We explored whether a tail could mitigate and compensate for these unfavorable dynamics. To do so, we built a RHex-inspired quadrupedal system and tested it over a terrain designed to elicit failure. Diverse terradynamic interactions, challenging to predict or detect in this environment, trapped the robot. However, a properly used active tail enhanced robot capabilities by mitigating such interactions, improving the traversal likelihood and freeing probability. Additionally, we found that improper usage hindered performance. In summary, an actuated tail with minimal control can be used to augment existing robots to aid locomotion over hazardous terrains. Future work could include a load-triggered tail-limb actuation,

where the limbs reverse as the tail makes ground contact. This could prevent the legs from being driven further into the walls when the tail lifts the device up, allowing the robot to leave the region of failure. Furthermore, the tail could be used for steering in concert with limb-based turning [10, 14].

Acknowledgements. We thank Simon Sponberg and GT IRIM for laboratory space, Yasemin Ozkan-Aydin and Frank Hammond for help in limb manufacturing. Funding for D.S. provided by NSF PoLS Student Research Network (grant no. PHY-1205878); for K.D. by GT NSF-Simons Southeast Center for Mathematics and Biology (grant no. DMS1764406, SFARI 594594), and D.I.G. by a Dunn Family Professorship.

References

1. Rebula, J.R., et al.: A controller for the littledog quadruped walking on rough terrain. In: Proceedings 2007 IEEE International Conference on Robotics and Automation, pp. 1467–1473 (2007)
2. Boston Dynamics: Spot, May 2021. <https://www.bostondynamics.com/spot>
3. Boston Dynamics: Atlas, May 2021. <https://www.bostondynamics.com/atlas>
4. Saranli, et al.: RHex: a simple and highly mobile hexapod robot. *IJRR* **20**(7), 616–631 (2001)
5. Moore, E.Z., et al.: Reliable stair climbing in the simple hexapod ‘RHex’. In: Proceedings 2002 IEEE International Conference on Robotics and Automation, vol. 3, pp. 2222–2227 (2002)
6. Spagna, et al.: Distributed mechanical feedback in arthropods and robots simplifies control of rapid running on challenging terrain. *Bioinspir. Biomim.* **2**(1), 9 (2007)
7. Ozkan-Aydin, Y., et al.: A systematic approach to creating terrain-capable hybrid soft/hard myriapod robots. In: 2020 3rd IEEE International Conference on Soft Robotics (RoboSoft), pp. 156–163. IEEE (2020)
8. Schiebel, P.E., Maisonneuve, M.C., Diaz, K., Rieser, J.M., Goldman, D.I.: Robophysical modeling of bilaterally activated and soft limbless locomotors. In: Vouloutsis, V., Mura, A., Tauber, F., Speck, T., Prescott, T.J., Verschure, P.F.M.J. (eds.) *Biomimetic and Biohybrid Systems. Living Machines 2020. Lecture Notes in Computer Science*, vol. 12413, pp. 300–311. Springer, Cham (2020). https://doi.org/10.1007/978-3-030-64313-3_29
9. Murphy, R.: Personal communication (2021)
10. Pullin, A.O., et al.: Dynamic turning of 13 cm robot comparing tail and differential drive. In: 2012 IEEE International Conference on Robotics and Automation, pp. 5086–5093 (2012)
11. Casarez, C., et al.: Using an inertial tail for rapid turns on a miniature legged robot. In: 2013 IEEE International Conference on Robotics and Automation, pp. 5469–5474 (2013)
12. Briggs, R., et al.: Tails in biomimetic design: Analysis, simulation, and experiment. In: 2012 IEEE/RSJ International Conference on Intelligent Robots and Systems, pp. 1473–1480 (2012)
13. Chang-Siuet, E., et al.: A lizard-inspired active tail enables rapid maneuvers and dynamic stabilization in a terrestrial robot. In: 2011 IEEE/RSJ International Conference on Intelligent Robots and Systems, pp. 1887–1894 (2011)
14. Casarez, C.S., Fearing, R.S.: Steering of an underactuated legged robot through terrain contact with an active tail. In: 2018 IEEE/RSJ International Conference on Intelligent Robots and Systems (IROS), pp. 2739–2746. IEEE (2018)

15. NASA: Pathfinder's rocky terrain (1997). Accessed 15 Apr 2021
16. Epstein: The buffalo news: historic chautauqua institution amphitheater demolished into pile of rubble, September 2016. Accessed 15 Apr 2021
17. Hildebrand, M.: The quadrupedal gaits of vertebrates. *BioScience* **39**(11), 766 (1989)
18. Sponberg, S., Full, R.: Neuromechanical response of musculo-skeletal structures in cockroaches during rapid running on rough terrain. *JEB* **211**(3), 433–446 (2008)
19. Jacoff, A., et al.: Stepfield pallets: repeatable terrain for evaluating robot mobility. In: *Proceedings of the 8th Workshop on Performance Metrics for Intelligent Systems*, pp. 29–34 (2008)